



Neural Network Configurations for Filtering of Feed Stream Noise from Oscillating Continuous Microbial Fermentations

Pratap Patnaik

*Institute of Microbial Technology
Sector 39-A, Chandigarh-160 036, India
E-mail: pratap@imtech.res.in*

Received: March 16, 2006

Accepted: April 6, 2006

Published: April 26, 2006

Abstract: *Some microbial systems exhibit sustained oscillations under certain conditions. The maintenance and the suppression of oscillations are both important in different situations. While oscillations are clearly identifiable in small bioreactors, the influx of noise fuzzifies the oscillations in larger vessels. So, noise-filtering devices are employed to recover clear oscillating profiles. Recent work has shown that an auto-associative (AA) neural network is a better than standard algorithmic filters. In this study, nine neural network designs are compared for their ability to filter Gaussian noise in the substrate inflow rate of a continuous fermentation containing *Saccharomyces cerevisiae*. While the AA network is the best overall, specific performance criteria favor other designs. Thus the choice of a neural filter depends on the evaluation criterion, which is guided by the application.*

Key words: *Microbial oscillations, *Saccharomyces cerevisiae*, Bioreactor, Noise inflow, Neural filters.*

Introduction

Many microbial processes exhibit sustained oscillations over long durations. Under controlled conditions, clear oscillations are observable. In more realistic natural environments and production processes, however, the influx of noise obfuscates the intrinsic oscillations from the aberrations caused by noise. Since the occurrence of oscillations is linked to the reactions inside the cells and to transport processes across the cell walls [22], the identification of the oscillating signals is important for the understanding and control of large bioreactors [6, 15, 34].

The bacterium *Zymomonas mobilis* and the yeast *Saccharomyces cerevisiae* have been the work-horses of most studies of oscillating phenomena. *S. cerevisiae* is more popular in view of its ease of cultivation, well-understood physiology and industrial importance [7, 22]. Two recent publications [23, 24] have addressed the issue of recovering smooth oscillations from noise-distorted concentration profiles during continuous fermentations with *S. cerevisiae*. Both studies were based on experimental observations [1, 7, 16, 27] that, in certain ranges of the dilution rate and the gas-liquid mass transfer rate of oxygen, continuous cultures of *S. cerevisiae* display oscillating profiles for some key concentrations such as those of the biomass, carbon substrate (glucose), product (ethanol), storage carbohydrate and dissolved oxygen. Different types of oscillations occur in different ranges of these two manipulated variables, and some oscillations may comprise a superposition of two or more simple unimodal oscillations of different amplitudes.



Investigations of the causes of oscillations in *S. cerevisiae* have concentrated on either of two classes of oscillations. Circadian oscillations are related to the cell cycle and have long time periods of several hours. Ultradian (metabolic) oscillations are not synchronized with the cell cycle and have shorter periods between a few minutes and a few hours. Both classes of oscillations have been discussed in terms of possible mechanisms and models [7, 13, 33]. The brief distinction outlined above should suggest that ultradian oscillations can be more readily controlled than circadian oscillations through external interventions without upsetting the cell cycle.

Therefore, from a bioengineering perspective, ultradian oscillations are of primary interest: (a) as a vehicle to study interactions between cellular control systems and environmental controls and (b) to regulate and optimize industrial fermentations, where oscillations are usually undesirable. In shake flasks and small bioreactors, homogeneous noise-free conditions can be maintained and the main objective usually is to obtain metabolic information. On progressing toward pilot- and production-scale bioreactors, the emphasis shifts to the generation of biomass or product, and environmental influences become pronounced. These influences are of two kinds. At one level, noise infiltrates a reactor along with the feed stream(s). This complicates measurements for data with discernible features, and it can seriously change bioreactor performance [14, 26]. The other influence is through deliberate manipulations of some variables, generally the flow (or dilution) rate of the main substrate or some concentration or the gas-liquid mass transfer rate, to achieve greater stability or higher productivity.

The latter influence depends partly on the former, in that important features of the fermentation should be clearly identifiable for suitable manipulatory responses. When the measured data are clouded by noise, it becomes difficult to identify the salient features and to derive useful quantitative information for control decisions. Therefore in the operation of large bioreactors, especially in continuous and fed-batch mode, proper abatement of the noise through filtering devices is essential to retrieve relatively clear signals characterizing the performance of the microbial culture.

In previous studies [22, 24] it was shown that an auto-associative (AA) neural network provided better filtering of noise-affected microbial oscillations than was possible with algorithmic filters such as the extended Kalman filter, the Butterworth filter and the moving average filter. However, neural architectures other than the AA network may also be used for modulation of noise inflow. Since it is difficult to specify *a priori* which design is the best, a library of neural networks has been created [18] for bioreactor applications. From the current version of this library, COMPARE, five basic architectures were selected. Their usefulness has been demonstrated both during the creation of COMPARE and recently for the fermentative production of poly- β -hydroxybutyrate [25]. In the latter study, two variants of the backpropagation network were used – with momentum and with adaptive learning. Here a combination of both variants has also been considered, as also the adoption of generalized regression with the radial basis network. In addition, the AA neural filter was also a candidate network, thus creating a set of nine network configurations as against seven in Patnaik [25]. Moreover, the present application focuses on an oscillating culture whereas the previous work was for a monotonic culture.



Fermentation description and data generation

In aerobic continuous fermentations, *S. cerevisiae* may exhibit monotonic, oscillatory or chaotic behavior with time [7, 24, 27]. The nature of the fermentation depends on a number of variables, such as pH, the carbon source, the dilution rate and the rate of oxygen transfer to the broth [1, 2, 11, 17, 27], but the latter two variables have greater influence and are therefore employed as manipulated variables for reactor control. Of these two, the dilution rate is preferred since it provides excellent regulatory performance and, owing to the greater sensitivity of the fermentation, it enables effective control actions through small changes [6, 10, 21]. Since the influx of noise is mainly through the liquid feed streams, the choice of this manipulated variable underlines the importance of proper filtering to obtain reliable signals for the control systems. It may be clarified here that while in batch fermentations the main product, ethanol, is produced only in the absence of oxygen, this is observed in certain ranges of the dissolved oxygen concentration for aerobic continuous cultures [2, 17, 27].

Published experimental data pertain to laboratory-scale bioreactors, which are elaborately controlled, homogeneous and noise-free. This is not true of pilot- and industrial-scale vessels, where process noise and its filtering can be significant for productivity and profitability. However, practical difficulties and commercial restrictions limit the availability and disclosure of industrial data. Under such limitations, many authors [4, 28, 29] have found it expedient to generate data mimicking industrial fermentations by adding noise to a bioreactor model based on laboratory-scale experiments, and solving the model under different operating conditions. This method also enables exploration of fermentation performance over wide ranges of conditions, which would be impractical or risky in an actual plant.

Consistent with earlier studies [22, 24], a model proposed by Jones and Kompala [11] was employed to generate simulated noisy data. The equations are presented in the Appendix. This model differs from many other models of *S. cerevisiae* fermentations in a fundamental way. Whereas most models are mechanistic, that of Jones and Kompala is cybernetic. Mechanistic models are derived in a manner similar to those for chemical reactions. In doing so, they ignore the fact that cells can be 'living' entities, with complex internal regulatory processes that enable them to assimilate past knowledge, make informed choices and adjust their responses so as to maximize their survival under the prevailing conditions [5].

On this basis, Jones and Kompala [11] postulated that in an aerobic continuous culture *S. cerevisiae* may follow any of three metabolic pathways: glucose fermentation, ethanol oxidation and glucose oxidation. Glucose is the main carbon source. Each pathway is controlled by a key enzyme, which is synthesized or repressed according to the prevailing conditions. A pivotal concept here is that the pathways are not mutually exclusive, so the cells may distribute the available resources among the pathways so as to promote their own survival. The pathways are thus constantly in a state of flux, and dynamic competition among them is, according to Jones and Kompala, the main cause of oscillations. Their cybernetic model is presented in the Appendix. It describes the rates of change of eight concentrations: biomass, glucose, ethanol, dissolved oxygen, a storage carbohydrate and the three key enzymes. However, the key enzymes are often difficult to identify and monitor. So, the first five variables are usually observed.

The cells may be induced to allocate the resources in any desired manner among the pathways by manipulating either the flow (or dilution) rate or, in aerobic fermentations, the rate of transfer of oxygen. The dilution rate is preferred because it is easier to change, evokes quicker

responses and has certain control advantages [6, 10, 21]. The substrate flow stream is also a major carrier of noise, and this makes it imperative to filter out the noise and recover stable oscillations. Previous studies [8, 19, 26] have shown that this noise may be modeled by a set of Gaussian distributions with a common mean equal to the instantaneous value of the flow rate and time-dependent variances. Details of the noise generation procedure are described elsewhere [20]; as in that work, the variances spanned 0 to 10% of the current mean values, which were obtained by solving the noise-free model in the Appendix. Then the model with noise was solved to obtain simulated ‘real’ data. Since noise is added to the substrate feed rate before the model is solved, it is systemic and not superimposed on the model.

Application and discussion

To cover oscillations of different amplitudes and frequencies, Jones and Kompala’s [11] model was solved, without and with noise, for a representative experiment in which they had maintained the dilution rate at $0,13 \text{ h}^{-1}$ for 0-100 h, and then increased it in two steps, first to $0,15 \text{ h}^{-1}$ until 200 h and then to $0,165 \text{ h}^{-1}$ until the end of the fermentation at 300 h. With each increase, oscillations in the concentrations of biomass, glucose, ethanol, dissolved oxygen and storage carbohydrates decreased in both amplitude and frequency.

From each time slice of 100 h, the data were sampled at hourly intervals. Then from each such set of 100 data, 70 points were chosen randomly to train the neural filters and 30 were used to test the filters. Since the choices were random, the two sub-sets of each data set had both intersections and extrapolation. This feature and the separate selection of data for each dilution rate ensured that the neural filters were tested for their extrapolation capability and for oscillations of different amplitudes and frequencies. While it is accepted that neural networks are good predictors of unseen data within the ranges of training, their ability to work well outside the training region is not always guaranteed [4, 31].

Based on earlier applications and the coverage of different architectures, the following five types of neural networks were selected from the COMPARE library [18]: (i) backpropagation (BP), (ii) radial basis (RB), (iii) auto-associative, (iv) Elman and (v) Hopfield. Three variants of the BP network were tested: the standard BP, BP with momentum (BPM) and BP with adaptive learning (BPAL). The RB network too was tested without and with generalized regression (RBG). All of these are described in the standard literature [9]. Although the data for each time slice and dilution rate were split in the ratio 7:3 for training and testing, all training data were combined and so were the test data. Two considerations motivated this decision. One was to remove any hidden bias that might be created by special (but unnoticed) features of a particular set. Secondly, a neural filter should be effective across a wide spectrum of conditions to be practically useful.

Each network was trained until a cumulative normalized mean squared error, CNMSE, reached less than 2%. The CNMSE is defined and explained below. Let y_{ij} be the j -th value of the i -th variable. Then,

$$\text{CNMSE (\%)} = 100 \sum_{i=1}^M \sum_{j=1}^N \left(\frac{y_{ij}^r - y_{ij}^f}{y_{ij}^r} \right)^2 \quad (1)$$

In Eq. (1), M is the number of variables and N the total number of training data. The superscript ‘r’ denotes a raw ‘experimental’ (or simulated) value, while ‘f’ denotes a filtered value. Obviously the raw data are for a bioreactor without a neural filter. Although the model in the Appendix has 8 concentrations, the three key enzymes are difficult to identify, isolate

and monitor. Moreover, practical interest is focused on the macroscopically measurable variables, which are the concentrations of biomass, glucose, ethanol, dissolved oxygen and storage carbohydrates. Therefore $M = 5$ and $N = 3 \cdot 70 = 210$.

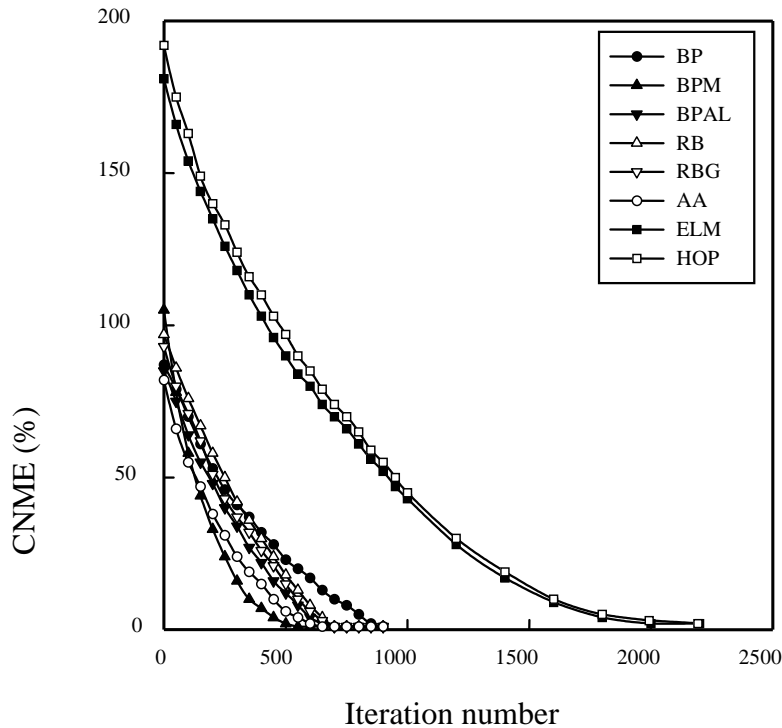


Fig. 1 Convergence profiles for different neural network configurations. BP-backpropagation, BPM-BP with momentum, BPAL-BP with adaptive learning, BPMA-BP with momentum and adaptive learning, RB-radial basis, RBG-RB with generalized regression, ELM-Elman, HOP-Hopfield.

Fig. 1 displays the convergence profiles during training of the neural filters. Each network was trained until the CNMSE (Eq. (1)) reached less than 2%. The final configurations of each of the filters are summarized in Table 1.

Table 1. Final configurations of different neural filters

Network type	Number of neurons of different types			
	Input	Recurrent	Hidden	Output
BP	5	0	4	5
BPM	5	0	4	5
BPAL	5	0	4	5
BPMA	5	0	4	5
RB	5	0	3	5
RBG	5	0	3	5
AA	5	0	3	5
ELM	5	5	4	5
HOP	5	5	4	5

BP with momentum is seen to converge the fastest, with AA and BP with adaptive learning following closely. Although the radial basis filter has one fewer neuron than the BP and AA types, its convergence is slower, partly because of its lower ability to distinguish between

good data and spurious data [9]. Thus, while an RB network may work efficiently with carefully selected data, it is less effective for on-line applications involving noisy or scattered data. The least efficiency of the Elman and Hopfield networks may not be surprising since their complex structures and information flows make them overdesigned and sluggish.

The effectiveness of the trained networks in filtering out noise in the glucose flow rate to restore noise-free oscillations is compared in Fig. 2 for the test data. The statistics in Fig. 2 are defined below. To have a common basis for comparison, the values reported are for the configurations obtained after 2400 iterations, this number being set by the convergence criterion of 2% for the worst filter.

Cumulative normalized mean error:

$$CNME (\%) = 100 \sum_{i=1}^M \sum_{j=1}^N \left(\frac{y_{ij}^r - y_{ij}^f}{y_{ij}^r} \right) \tag{2}$$

Cumulative normalized standard deviation of errors:

$$CNSDE (\%) = \frac{100}{N-1} \sum_{i=1}^M \sum_{j=1}^N \left[\left(\frac{y_{ij}^r - y_{ij}^f}{y_{ij}^r} - \bar{y}_i \right)^2 \right] \tag{3}$$

Equation (3) extends the standard definition of the standard deviation to a sequence of M variables. Thus, \bar{y}_i is the mean error for the i-th variable, calculated as:

$$\bar{y}_i = \sum_{j=1}^N \left(\frac{y_{ij}^r - y_{ij}^f}{y_{ij}^r} \right) \tag{4}$$

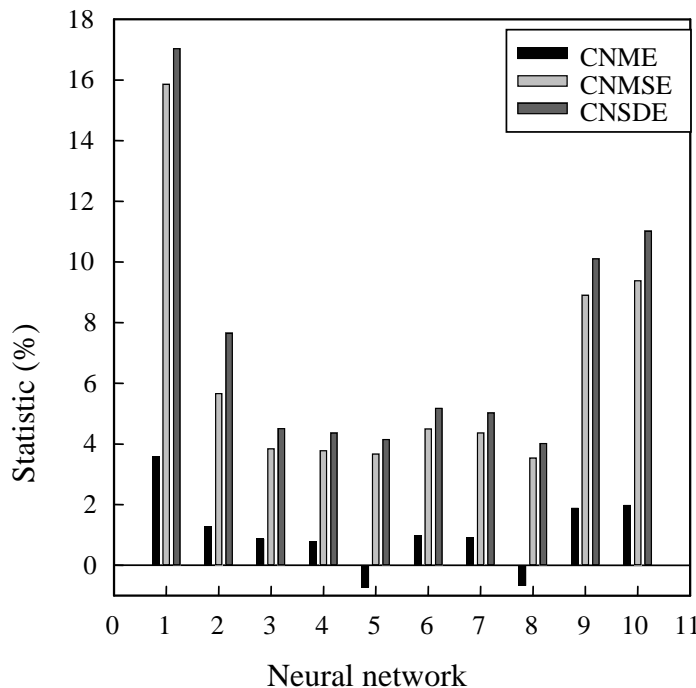


Fig. 2 Statistical comparisons of different neural filters.
 1-BP, 2-BPM, 3-BPAL, 4-BPMA, 5-RB, 6-RBG,
 7-AA, 8-ELM, 9-HOP

The cumulative normalized mean squared error, CNMSE (%), has been defined in Eq. (1). While all three statistics show that the auto-associative neural network is the most effective filter, the order of the other filters differs from that of their convergence efficiencies (Fig. 1). The BP network, which converged fastest, is a relatively poor filter, and the addition of momentum and adaptive learning improve its performance considerably. The inclusion of both these features make BPMA nearly as good as an AA filter but slow down its convergence. These two filters also differ from the others in another aspect. The CNME is negative for AA and BPMA filters and positive for the others. Unlike the CNME, the CNMSE and the CNSDE are always positive and the latter measures the spread of the errors. So, the contrasting signs of the CNME and the other two statistics, together with the smaller values of all three measures, suggest that the errors for the AA and BPMA filters are equally distributed in a narrow band on either side of the zero error line. Likewise, the larger statistics, all with positive sign, indicate larger errors that have a skewed distribution, implying poor filtering of noise by the other neural configurations. The values without any filter are understandably the largest because real noise has a skewed Gaussian distribution [4, 26].

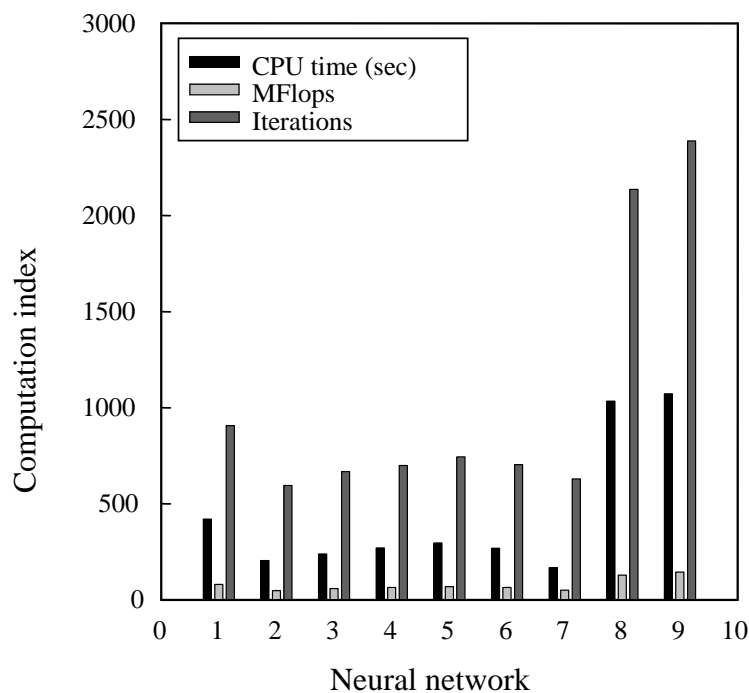


Fig. 3 Comparisons of computation indexes for different neural filters. The identification numbers of the neural networks are explained in Fig. 2

A good filter should ideally be fast and efficient. The speeds of restoring noise-affected oscillations to within 2% (in terms of CNME) of the noise-free oscillations are compared in Fig. 3. An interesting contrast with Fig. 2 is that the relative merits of different neural architectures differ from one metric to another. The AA network converges fastest in terms of CPU time but requires more iterations and floating point operations (flops) than the BPM. Although adaptive learning enables a BP filter to reduce the inflow of noise sufficiently to bring the oscillating profiles within 0,8% of the noise-free profiles, this also slows down convergence. Therefore, as might be expected, the inclusion of both momentum and adaptive learning reduces speed of convergence but improves the closeness between the noise-free and noise-filtered outputs.



The Elman and Hopfield networks are both recurrent networks. The presence of recurrent neurons and the feedback of signals make these architectures good predictors of time-dependent variables but not good modulators [9]. So these networks can accurately learn, reproduce and predict concentration profiles of bioreactors, even in the presence of disturbances [18-20], but are inefficient in filtering out the disturbances. While their complexity may make them robust enough to overcome discontinuities, it also slows down their learning speed, as with BPMA. Moreover, Hopfield designs may have spurious stable points that lead to incorrect results [9].

Conclusions

Under certain operating conditions *S. cerevisiae* exhibits sustained oscillating outputs in continuous cultures. The occurrence and the nature of the oscillations follow complex dynamics [7, 32], which may be controlled by manipulating the pH, the dissolved oxygen concentration and the dilution rate; of these the dilution rate is the preferred variable.

The involvement of a network of reactions in the metabolic system results in both non-oscillating steady states and oscillating states being possible at the same set of conditions [3, 33]. This has two implications. One is that the final state depends on the initial conditions and the path the unsteady system follows. The second implication is that disturbances, such as noise in a feed stream, may displace the fermentation from a steady (non-oscillating) state to an oscillating state or vice versa. Depending on the current state and its sensitivity [21], noise carried by the feed stream may be sufficient to displace the fermentation from one state to another. This may pose serious problems in process dynamics and control [15, 34], and hence it is practically important to filter out the inflow of noise for stable and efficient operation.

Previous studies [22, 24] have shown that an AA neural network provides better filtering than commonly used algorithmic filters such as the extended Kalman and cusum filters. However, neural architectures other than the AA network are possible. To evaluate their effectiveness, nine different neural filters were compared in terms of different performance indexes. While the AA was the best overall, other configurations were superior for individual criteria. This observation suggests that the choice of a neural noise filter depends on the relative importance of different measures of performance, which are guided by the intended application. Nevertheless, all neural filters were superior to algorithmic filters.

Nomenclature

C	intra-cellular storage carbohydrate concentration, [g g ⁻¹ biomass]
D	dilution rate, [h ⁻¹]
e _i	key enzyme concentration for i-th pathway, [g g ⁻¹ biomass]
E	ethanol concentration, [g l ⁻¹]
G	glucose concentration, [g l ⁻¹]
G ₀	inlet glucose concentration, [g l ⁻¹]
K _i	Michaelis constant for i-th pathway, [g l ⁻¹]
K _{o₂}	saturation constant for ethanol oxidation, [mg l ⁻¹]
K _{o₃}	saturation constant for glucose oxidation, [mg l ⁻¹]
k _{La}	oxygen mass transfer coefficient, [h ⁻¹]
O	dissolved oxygen concentration, [mg l ⁻¹]
O*	dissolved oxygen solubility limit, [mg l ⁻¹]



r_i	cell growth rate for i-th pathway, [h ⁻¹]
S_i	carbon substrate concentration for i-th pathway, [g l ⁻¹]
t	time, [h]
u_i	i-th pathway cybernetic variable controlling enzyme synthesis, [-]
v_i	i-th pathway cybernetic variable controlling enzyme activity, [-]
X	cell mass concentration, [g l ⁻¹]
Y_i	yield coefficient for i-th pathway, [g biomass g ⁻¹ substrate]
Greek letters	
α	specific enzyme synthesis rate, [h ⁻¹]
α^*	constitutive enzyme synthesis rate, [h ⁻¹]
β	specific enzyme degradation rate, [h ⁻¹]
ϕ_i, γ_i	stoichiometric parameters, [g g ⁻¹]
μ_i	specific growth rate for i-th pathway, [h ⁻¹]
$\mu_{i,max}$	maximum specific growth rate for i-th pathway, [h ⁻¹]

Appendix

Jones and Kompala [11] extended an earlier model [12] to include variations in dissolved oxygen concentration. Previous studies have shown that, with glucose as the main carbon source, there are three metabolic pathways. One is glucose fermentation, which produces a high growth rate and ethanol production. The second pathway is followed when glucose concentration is low; here the cells consume ethanol oxidatively. While these two metabolic routes are common to both batch and continuous cultures, a third, glucose oxidation, is observed only in continuous operation. According to Jones and Kompala [11], the pathways follow Monod kinetics.

(a) Glucose fermentation

$$r_1 = \mu_1 e_1 \left(\frac{G}{K_1 + G} \right) \quad (A1)$$

(b) Ethanol oxidation

$$r_2 = \mu_2 e_2 \left(\frac{E}{K_2 + E} \right) \left(\frac{O}{K_{O_2} + O} \right) \quad (A2)$$

(c) Glucose oxidation

$$r_3 = \mu_3 e_3 \left(\frac{G}{K_3 + G} \right) \left(\frac{O}{K_{O_3} + O} \right) \quad (A3)$$

As seen above, each pathway has a ‘key enzyme’, e_1 or e_2 or e_3 . The cybernetic method postulates that the growth rate r_i along a metabolic path is maximized when two sets of cybernetic variables, u_i and v_i ($i = 1, 2, 3$), follow the equations given below. Kompala et al.’s [12] paper may be consulted for detailed explanation of the basis of these equations.



$$u_i = \frac{r_i}{\sum_j r_j}; \quad i = 1, 2, 3 \quad (\text{A4})$$

$$v_i = \frac{r_i}{\max_j r_j}; \quad i = 1, 2, 3 \quad (\text{A5})$$

Briefly, the u_i 's control the enzyme synthesis rates and the v_i 's govern their activities. Kompala et al. [12] identified 8 key variables. These were the concentrations of cell mass, glucose, ethanol, oxygen and intra-cellular carbohydrate, and the activities of the three key enzymes. Storage carbohydrates, notably trehalose and glycogen, are accumulated inside the cells when there is deficiency of glucose and ethanol, and they are consumed if either of these substrates is present in appreciable quantities. In a continuous culture, the dynamic mass balances for these variables follow the equations given below [11].

$$\frac{dX}{dt} = \left(\sum_i (r_i v_i) - D \right) X \quad (\text{A6})$$

$$\frac{dG}{dt} = (G_0 - G)D - \left(\frac{r_1 v_1}{Y_1} + \frac{r_3 v_3}{Y_3} \right) X - \phi_4 \left(C \frac{dX}{dt} + X \frac{dC}{dt} \right) \quad (\text{A7})$$

$$\frac{dE}{dt} = -DE + \left(\phi_1 \frac{r_1 v_1}{Y_1} - \frac{r_2 v_2}{Y_2} \right) X \quad (\text{A8})$$

$$\frac{dO}{dt} = k_L a (O^* - O) - \left(\phi_2 \frac{r_2 v_2}{Y_2} + \phi_3 \frac{r_3 v_3}{Y_3} \right) X \quad (\text{A9})$$

$$\frac{de_i}{dt} = \alpha u_i \frac{S_i}{K_i + S_i} - \left(\sum_j (r_j v_j) + \beta \right) e_i + \alpha^* \quad (\text{A10})$$

$$\frac{dC}{dt} = \gamma_3 r_3 v_3 - (\gamma_1 r_1 v_1 + \gamma_2 r_2 v_2) C - \sum_i (r_i v_i) C \quad (\text{A11})$$

The term α^* in Eq. (A10) was included on the recommendation of Turner and Ramkrishna [30], who showed that a small constitutive synthesis term was required in order to predict correctly the induction of enzymes that have been repressed for long durations.

The model is completed by adding the equations for the specific growth rates contained in Eqs. (1 – 3).

$$\mu_i = \mu_{i,\max} \left(\frac{\mu_{i,\max} + \beta}{\alpha + \alpha^*} \right) \quad (\text{A12})$$

References

1. Beuse M., R. Bartling, A. Kopmann, H. Diekmann, M. Thoma (1998). Effect of Dilution Rate on the Mode of Oscillation in Continuous Cultures of *Saccharomyces Cerevisiae*, J. Biotechnol., 61, 15-31.



2. Beuse M., A. Kopmann, H. Diekmann, M. Thoma (1999). Oxygen, pH Value, and Carbon Source Induced Changes of the Mode of Oscillation in Synchronous Continuous Culture of *Saccharomyces Cerevisiae*, *Biotechnol. Bioeng.*, 63, 410-417.
3. Chen C. I., K. A. McDonald, L. Bisson (1990). Oscillating Behavior of *Saccharomyces Cerevisiae* in Continuous Culture. I. Effects of pH and Nitrogen Levels, *Biotechnol. Bioeng.*, 36, 19-27.
4. Chen V. C. P., D. K. Rollins (2000). Issues Regarding Artificial Neural Network Modeling for Reactors and Fermenters, *Bioproc. Biosyst. Eng.*, 22, 85-93.
5. Dhurjai P., D. Ramkrishna, C. Flickinger, G. T. Tsao (1985). A Cybernetic View of Microbial Growth: Modeling Cells as Optimal Strategists, *Biotechnol. Bioeng.*, 27, 1-9.
6. Dochain D., M. Perrier (1997). Dynamic Modeling, Analysis, Monitoring and Control Design for Nonlinear Bioprocesses, *Adv. Biochem. Eng. Biotechnol.*, 56, 147-197.
7. Duboc Ph., I. Marison, U. von Stochar (1996). Physiology of *Saccharomyces Cerevisiae* during Cell Cycle Oscillations, *J. Biotechnol.*, 51, 57-72.
8. Glassey J., G. A. Montague, A.C. Ward, B. V. Kara (1994). Artificial Neural Network based Experimental Design Procedures for Enhancing Fermentation Development, *Biotechnol. Bioeng.*, 44, 397-405.
9. Hassoun M. H. (1995). *Fundamentals of Artificial Neural Networks*, MIT Press, Cambridge, MA.
10. Henson M. A., D. E. Seborg (1992). Nonlinear Control Strategies for Continuous Fermenters, *Chem. Eng. Sci.*, 47, 821-835.
11. Jones K. D., D. S. Kompala (1999). Cybernetic Model of the Growth Dynamics of *Saccharomyces cerevisiae* in Batch and Continuous Cultures, *J. Biotechnol.*, 71, 105-131.
12. Kompala D. S., D. Ramkrishna, G. T. Tsao (1984). Cybernetic Modeling of Microbial Growth on Multiple Substrates, *Biotechnol. Bioeng.*, 26, 1272-1281.
13. Lloyd D. (1998). Circadian and Ultradian Clock-controlled Rhythms in Unicellular Organisms, *Adv. Microb. Physiol.*, 39, 291-338.
14. Lubbert A., S. B. Jorgensen (2001). Bioreactor Performance: A More Scientific Approach for Practice, *J. Biotechnol.*, 85, 187-212.
15. Martegani E., D. Porro, B. M. Ranzi, L. Alberghina (1990). Involvement of Cell Size Control Mechanism in the Induction and Maintenance of Oscillations in Continuous Cultures of Budding Yeast, *Biotechnol. Bioeng.*, 36, 453-459.
16. Murray D. B., S. Roller, H. Kuriyama, D. Lloyd (2001). Clock Control of Ultradian Respiratory Oscillation Found during Yeast Continuous Culture, *J. Bacteriol.*, 183, 7253-7259.
17. Parulekar S. J., G. B. Semones, M. J. Rolf, J. C. Lievense, H. C. Lim (1986). Induction and Elimination of Oscillations in Continuous Cultures of *Saccharomyces Cerevisiae*, *Biotechnol. Bioeng.*, 28, 700-710.
18. Patnaik P. R. (1996). Preliminary Screening of Neural Network Configurations for Bioreactor Applications, *Biotechnol. Techniques*, 10, 967-970.
19. Patnaik P. R. (1999). Neural Control of an Imperfectly Mixed Fed-batch Bioreactor for Recombinant β -galactosidase, *Biochem. Eng. J.*, 3, 113-120.
20. Patnaik P. R. (1999). Improvement of the Microbial Production of Streptokinase by Controlled Filtering of Process Noise, *Process Biochem.*, 35, 309-315.
21. Patnaik P. R. (2001). A Sensitivity Approach to Manipulated Variable Selection for Control of a Continuous Recombinant Fermentation, *Chem. Eng. Sci.*, 56, 3311-3314.
22. Patnaik P. R. (2003). On the Performances of Noise Filters in the Restoration of Oscillatory Behavior in Continuous Yeast Cultures, *Biotechnol. Lett.*, 25, 681-685.



23. Patnaik P. R. (2003). Oscillatory Metabolism of *Saccharomyces cerevisiae*: An Overview of Mechanisms and Models, *Biotechnol. Adv.*, 21, 183-192.
24. Patnaik P. R. (2004). A Lyapunov Comparison of Noise-filtering Methods for Oscillating Yeast Cultures, *A. I. Ch. E. J.*, 50, 1640-1647.
25. Patnaik P. R. (2005). Neural Network Designs for Poly- β -hydroxybutyrate Production Optimization under Simulated Industrial Conditions, *Biotechnol. Lett.*, 27, 409-415.
26. Rohner M., H. P. Meyer (1995). Application of Modeling for Bioprocess Design and Control in Industrial Production, *Bioproc. Eng.*, 13, 69-78.
27. Satroutdinov A. D., H. Kuriyama, H. Kobayashi (1992). Oscillatory Metabolism of *Saccharomyces cerevisiae* in Continuous Culture, *FEMS Microbiol. Lett.*, 98, 261-268.
28. Simutis R., A. Lubbert (1997). Exploratory Analysis of Bioprocesses using Artificial Neural Network Based Methods, *Biotechnol. Prog.*, 13, 479-487.
29. Tian Y., J. Zhang, A. J. Morris (2002). Optimal Control of a Fed-batch Bioreactor Based upon an Augmented Recurrent Neural Network Model, *Neurocomputing*, 48, 919-936.
30. Turner B. G., D. Ramkrishna (1988). Revised Enzyme Synthesis Rate Expression in Cybernetic Models of Bacterial Growth, *Biotechnol. Bioeng.*, 31, 41-43.
31. van Can H. J. L., H. A. B. te Braake, C. Helliga, K. C. A. M. Luyben, J. J. Heijnen (1997). An Efficient Model Development Strategy for Bioprocess Based on Neural Networks in Macroscopic Balances, *Biotechnol. Bioeng.*, 54, 549-566.
32. Wolf J., H-Y. Sohn, R. Heinrich, H. Kuriyama (2001). Mathematical Analysis of a Mechanism for Autonomous Metabolic Oscillations in Continuous Culture of *Saccharomyces cerevisiae*, *FEBS Lett.*, 499, 230-234.
33. Zamamiri A. M., G. Birol, M. A. Hjortso (2001). Multiple Steady States and Hysteresis in Continuous Oscillating Cultures of Budding Yeast, *Biotechnol. Bioeng.*, 75, 305-312.
34. Zhang Y., A. M. Zamamiri, M. A. Henson, M. A. Hjortso (2002). Cell Population Models for Bifurcation Analysis and Nonlinear Control of Continuous Yeast Bioreactors, *J. Process Control*, 12, 721-734.